



## Ag doped MnOx catalyst for formaldehyde removal at room temperature

Munzar Badshah<sup>\*</sup>, Shozab Mehdi, Imran Abbas, Saqib Mujtaba, Muhammad Usman,  
Kamran Alam

Ghulam Ishaq Khan Institute of Engineering Sciences and Technology, Topi, Pakistan

<sup>\*</sup>Corresponding Author E-mail: munzar.khan11@gmail.com

### ABSTRACT

The abundant amount of formaldehyde gas in the indoor public places from the building materials such as furniture, and consumables have a severe health effect on the human. Research indicated that long-term exposure to such an environment even with a low concentration of less than 0.5 ppm can damage the central nervous system and cause severe carcinogenic effects. Therefore, it is vital to develop such a method that can oxidize the formaldehyde at ambient temperature. Here in this research work, a novel ambient temperature metal oxide catalyst (MnOx) was synthesized with silver doping to enhance its efficiency and activity. The said catalyst was synthesized using the Co-precipitation method at pH 7 and calcined at 450°C. Doping the catalyst with Ag enhanced the surface area and crystallinity of the catalyst which in turn improved the efficiency of the prepared catalyst. Thermal stability, crystallinity, and surface area were analyzed using TGA/DSC, XRD, and BET respectively. The surface area of undoped MnO<sub>2</sub> was increased from 27.431 m<sup>2</sup> g<sup>-1</sup> to 33.481 m<sup>2</sup> g<sup>-1</sup> for the doped MnOx catalyst. Formaldehyde was tested at ambient temperature in the elongated reactor with a diameter of 0.5 inches and length of 5 inches. The initial concentration of Formaldehyde taken in the reactor was 20 ppm. The removal efficiency of Undoped MnO<sub>2</sub> was 83% efficiency while the Ag-doped MnOx catalyst removal efficiency was 94%. The enhanced efficiency was due to the higher surface area and higher crystallinity of the doped catalyst. The present work thus exploited an inexpensive approach to enhance the catalytic activity of transition metal oxides via doping them with a suitable metal.

### Keywords:

Formaldehyde  
MnO<sub>2</sub>  
Catalytic oxidation  
Co-precipitation

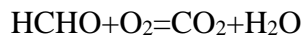
### 1. Introduction

Indoor air pollution's health effects have garnered considerable attention currently, especially because of our mostly spending time in indoors working. Indoor volatile organic compounds (VOCs) such as formaldehyde (HCHO), acetaldehyde, and toluene, which are released by household and decorating materials, are now the most significant indoor hazards. HCHO seems to be the most abundant and severe indoor air contaminant among them[1][3]. Unfortunately, both people and animals are very poisonous to HCHO. Ingestion of 30 mL of a solution containing 37 percent formaldehyde, regardless of how HCHO is consumed, has been

documented to cause mortality in an adult person, according to a study by the Agency for Toxic Substances and Disease Registry. People would experience nasal tumors, eye and skin inflammation, and nasopharyngeal cancer if exposed to HCHO for an extended period, even at a low concentration of a few ppm. At around 0.5 ppm, people start to feel eye discomfort. As a result, in 1977, the German Federal Agency of Health suggested a recommendation maximum value of 0.1 ppm in air to restrict human exposure in buildings[3], [4].

To avoid long-term health effects, WHO recommendations recommend a short-term HCHO exposure limit of 0.1 mg/m<sup>3</sup> and a long-term exposure limit of 0.2 mg/m<sup>3</sup> [2]. Various detoxification approaches have been investigated to eliminate formaldehyde from ambient air, including physical adsorption, chemical adsorption, photocatalytic oxidation (PCO), catalytic oxidation (thermal and non-thermal), Plasma catalytic oxidation, and biotechnical breakdown. However, they have a few flaws that prevent them from being used indoors: Adsorption is the most basic technique, with a high rate of elimination, high efficiency, and cheap cost however adsorbents have limited capabilities and must be replaced on a regular basis, when cleaning indoor pollutants. Under specific temperature and pressure, a porosity sorbent was used to achieve adsorption. When employed without strategy modification, traditional sorbents' sorption performance of FA is typically poor due to high fugacity (i.e., greater vapor pressure: 3883 mmHg) [5]. Plasma-catalytic and photocatalytic oxidation techniques, on the other hand, require additional energy input and plasma- or light-generation equipment's. This complicates the procedure and raises the footprint expenses significantly[2], [3]. Hazardous byproducts may also be produced by PCO and plasma. In alternative biological breakdown [6], the life cycle of microbes is still an issue that might impact purifying effectiveness. Because of its high removal efficiency, energy savings, and moderate reaction conditions, catalytic oxidation is the most promising of these methods. The removal of formaldehyde by catalytic oxidation using catalysts has recently been described. Among the methods, room-temperature catalytic oxidation is thought to be the most cost-effective, easy, and comprehensive method for removing HCHO. Room temperature catalytic oxidation does not demand UV light or plasma, and the catalyzed process takes place throughout the catalyst rather than only on the UV-activated surface. Because of these benefits, it is more suited for indoor formaldehyde elimination than other methods[3], [7],[8]. The development of high-efficiency catalysts to maintain reaction at ambient temperature is a crucial enabling element for room-temperature HCHO degradation. Catalytic oxidation can convert HCHO to H<sub>2</sub>O and CO<sub>2</sub>

completely without the formation of hazardous by-products or secondary pollutants. This can be done at ambient temperature, especially with noble metal catalysts, making it the most potential HCHO elimination method[9]. The overall reaction of this method is represented as reaction[10].



The development of high-efficiency catalysts to maintain reaction at ambient temperature is a crucial enabling element for room-temperature HCHO degradation. Different catalytic oxidation catalysts, such as metal oxides, supported non-noble metals, and supported noble metals on metal oxides, have been studied for their HCHO removal efficiency. As the advancement of catalytic oxidation methods is critical. Many significant studies on HCHO removal catalytic materials have been published. Supported noble metal on metal oxide catalyst and transition metal oxide catalyst are the two most common types. Transition-metal oxides have received a lot of interest because they are inexpensive, abundant, and have high thermal stability. A variety of meso/macroporous metal oxide catalysts have also been investigated for catalytic removal of HCHO [1]–[5], [11], [12]. Some of the currently, the oxide-supported noble metal catalytic materials (Ag, Pt, Pd and Au) used in catalytic removal of formaldehyde such as Ag/Co<sub>3</sub>O<sub>4</sub> [13], Ag/SBA-15 [14], Ag/Beta-Si[15], Ag/HMO[16], Ag/CeO<sub>2</sub>[17], Ag/MnO<sub>x</sub>-CeO<sub>2</sub>[18] Pt/MnO<sub>x</sub>-CeO<sub>2</sub>[19], Pt/TiO<sub>2</sub>[20], Pt/MnO<sub>2</sub>, Pt/Fe<sub>2</sub>O<sub>3</sub>[20], Pt/SiO<sub>2</sub>[21], PdMn/Al<sub>2</sub>O<sub>3</sub>[22], Pd/TiO<sub>2</sub>[23], Pd/Beta[24], Au/Fe<sub>2</sub>O<sub>3</sub>[25], Au/ZrO<sub>2</sub>[26], Au/CeO<sub>2</sub>[27], Au/Co<sub>3</sub>O<sub>4</sub>-CeO<sub>2</sub>[28]. A number of metal oxide catalysts for the removal of Formaldehyde have also been developed, including MnO<sub>x</sub>-SnO<sub>2</sub>[29], Co-Mn[30], KxMnO<sub>2</sub>[31], MnO<sub>x</sub>-CeO<sub>2</sub>[32].

Supported transition metal oxide catalysts, such as VO<sub>x</sub>, MnO<sub>x</sub>, and WO<sub>x</sub>, have been used frequently and efficiently in recent investigations.[38].Manganese oxide materials have the highest efficiency among these transition metal oxides catalysts due to their exceptional oxygen storage capability and appealing properties (e.g., favorable porous structure, large surface area, and tunability pore diameter) for improved gaseous VOC removal (e.g., FA). Even at ambient temperature, manganese oxide proved successful in removing formaldehyde, resulting in the selective generation of carbon dioxide and other gases, with no hazardous by-product gases produced. As a result, without the need of heat or electric energy, this metal oxide can be employed as an active component in the elimination of formaldehyde [2], [9]. In a static reaction tank, Sekine *et al.* first catalytically oxidized HCHO across various metal oxides (Ag<sub>2</sub>O, PdO, MnO<sub>2</sub>, TiO<sub>2</sub>, and CeO<sub>2</sub>), with MnO<sub>2</sub> exhibiting the highest removal efficiency, oxidizing high percentage of

formaldehyde at room temperature and suggesting that  $\text{MnO}_2$  might be employed as an active component in the elimination of HCHO from indoor air. [33]. Pyrolusite (0.23 nm x 0.23 nm), cryptomelane (0.46 nm x 0.46 nm), and todorokite (0.46 nm x 0.46 nm) are three manganese oxides developed by Chen et al. with varied square tunnel dimensions. Cryptomelane's effective tunnel diameter is the same as the dynamic diameter of the HCHO molecule, which may account for its exceptional catalytic activity [34]. However, several disadvantages, including as poor stability, and agglomeration prohibit more widespread use. Manganese oxides and manganese composite oxides, also have a low HCHO removal efficiency at low temperatures. As a result, despite their potential and cheap prices, there are limitations to indoor HCHO removal [24]. Since, because most practical catalytic processes are so complex that single component catalysts struggle to fulfill the challenges for superior efficiency, such as high activity, notable selectivity, and higher deactivation resistance, composite catalysts, which integrate two or more materials, are much more researched and used[2], [3], [12], [44].

The benefits of noble metal nanoparticles (NPs) based catalysts in heterogeneous catalysis for VOC degradation have recently been identified[45]–[47]. The advantages of dispersing noble metal NPs on supports include increase the number of surface atoms and therefore active sites, providing synergistic activity between the NP and the support, avoiding NP agglomeration even at relatively high particles densities, and decreasing the cost of catalysts[48]. Because of their increased activity for the break of C-C link, and C-H bonds, noble metals such as Pt, Au, and Ag are used and improve the oxidation of VOCs and boost the anti-toxicity of the catalyst, according to recent articles[38]. For example, according to Xuehua Yu., the improved Pt/ $\text{MnO}_2$  catalyst's strong metal-support interaction, widely dispersed Pt nanoparticles with tiny particle sizes, and high surface area resulted in increased formaldehyde oxidation activity.[24]. Similarly, Li et al. synthesis Au/  $\text{CeO}_2$  catalysts with a large specific surface area (261  $\text{m}^2 \text{g}^{-1}$ ) and high Au loading (5 wt% notional; 3 wt% measured) that converted 500 ppm HCHO to 92 percent at 37 °C. The large specific surface area of the  $\text{CeO}_2$  support supplied more oxygen vacancies as catalytic active sites, making the stimulation of adsorbed  $\text{O}_2$  molecules simpler[49]. Ag-supported catalysts, which are significantly less costly than the noble metals listed above, have been shown to exhibit effective low-temperature catalytic activity for HCHO oxidation, according to current research. On the Sigma-Aldrich website, the price of Pt per gram for  $\text{H}_2\text{PtCl}_6 \cdot 6\text{H}_2\text{O}$  is nearly 20 times that of Ag per gram for  $\text{AgNO}_3$ . At temperatures as low, full oxidation of HCHO was achieved over

Ag/MnO<sub>x</sub>-CeO<sub>2</sub> catalysts; the catalysts were produced using a deposition precipitation technique[18]. Preparing atomically dispersed metal catalysts, which theoretically have the greatest metal dispersion (i.e., 100 percent) and may offer numerous active sites for catalytic reaction, is another efficient method for increasing the activity of Ag-based HCHO oxidation catalysts. For example, silver nanoparticles supported on Hollandite-type manganese oxide nanorods demonstrated good activity for HCHO oxidation, according to Huang *et al.* With an initial HCHO concentration of 400 ppm, the conversion was 100 percent at 383K [15]. Because of the development of strong metal-metal contacts between Ag and Co, Qu *et al.* described a bimetallic AgCo/APTES@MCM-41 catalyst that could accomplish full oxidation of HCHO at temperatures as low as 90 °C. Due to increased surface OH supplied by K<sup>+</sup> ions, Bai *et al.* reported that K-Ag/Co<sub>3</sub>O<sub>4</sub> revealed full conversion of HCHO at 70 C[13]. He and Zhang experimented with a variety of supports (TiO<sub>2</sub>, Al<sub>2</sub>O<sub>3</sub>, and CeO<sub>2</sub>) and determined that the Ag/TiO<sub>2</sub> catalyst had the greatest catalytic performance (100 percent HCHO conversion at 95 °C) [42]. However, as compared to other noble metal catalysts, the performance of Ag-supported catalysts at room temperatures still needs to be improved.

Doping the Ag and measuring the HCHO removal efficiency at room temperature are critical since supported Ag catalysts have such a broad range of application.

In this study, we used a co-precipitation technique to produce Ag-based catalysts with MnO<sub>x</sub> supports, and then evaluated their performance for catalytic oxidation of HCHO at room temperature to that of undoped MnO<sub>x</sub>. On the two catalysts, a significant variation in catalytic activity was detected. With a gas hourly space velocity of 32000, Ag/MnO<sub>x</sub> had the best activity, recording 91 percent conversion of 110ppm HCHO at ambient temperature. The catalysts were then characterised by X-ray diffraction (XRD), TGA/DSC, and Brunauer-Emmett-Teller (BET). The intrinsic laws affecting the activity of Ag-based catalysts were explored and explained based on the findings.

## 2. Materials and methods

### 2.1. Catalyst preparation

Mn(NO<sub>3</sub>)<sub>2</sub>, AgNO<sub>3</sub>, and Na<sub>2</sub>CO<sub>3</sub> were chosen as raw materials for the AgMnO<sub>x</sub> catalysts, which were made via a co-precipitation technique. The following is the synthesis procedure for Ag/MnO<sub>x</sub>

catalysts; In 1000 ml of distilled water, make a 1 molar solution of  $\text{Mn}(\text{NO}_3)_2$  with a molecular mass of 178.95 g. Similarly, make a 0.1 molar  $\text{AgNO}_3$  solution by dissolving 0.124 g in 7.3 ml distilled water. For  $\text{Ag/MnO}_x$ , dissolve 7.3 mL of 0.1 M  $\text{AgNO}_3$  solution in 90 mL  $\text{Mn}(\text{NO}_3)_2$  solution under stirring to get homogeneous solution A; 105.988 g of  $\text{Na}_2\text{CO}_3$  was dissolved in 1000 mL deionized water under stirring to obtain homogeneous solution B. Pour the combination A into a funnel, then the solution B into a second funnel. In a beaker, add 100 mL distilled water and dropwise add both mixtures A and B, maintaining a pH of 7-8 with the digital pH meter along the continuous string. As the reaction proceeded, a mixed precipitate of  $\text{MnCO}_3$  and  $\text{Ag}_2\text{CO}_3$  was formed. Add  $\text{Na}_2\text{CO}_3$  solution until solution combination A is completed finish. The pH of the supernatant liquor was around 8. The precipitates were then put to a Buchner funnel and filtered, then washed until the pH of the solute was constant, then dried in an oven at  $100^\circ\text{C}$  for 12 hours and calcined at  $450^\circ\text{C}$  for 4 hours.  $\text{Ag/MnO}_x$  was the term given to the above-mentioned catalysts. Similarly, for  $\text{MnO}_x$  catalyst preparation same method is used without adding  $\text{AgNO}_3$ .

## 2.2. Catalyst characterization

The thermostability of precipitates was evaluated using a thermal gravimetric analyzer/dynamic stability control STARE system (TGA/DSC 1 STARE system, METTLER TOLEDO, Switzerland) at a  $20^\circ\text{C}/\text{min}$  heating rate from  $0^\circ\text{C}$  to  $900^\circ\text{C}$  under 50 mL/min of flowing argon gas.  $\text{MnCO}_3$  and  $\text{Ag}_2\text{CO}_3$ -containing precipitates made comprised the test sample. The crystalline structure of catalysts was determined using Xray powder diffraction (XRD) (D8-Advance, Bruker, Germany) with Cu K (wavelength = 0.15406 nm) radiation at a tube voltage of 40 kV and current of 40 mA in the  $2\theta$  range  $10\text{--}80^\circ$  with a step size of 0.05. The specific surface area and pore structure of the catalysts were determined using a Quantachrome physisorption analyzer (Autosorb-iQ-1MP, Quantachrome, USA). Before measuring, the catalysts were degassed for 6 hours at  $280^\circ\text{C}$ . The surface area (SBET) was calculated using data from the 0.05–0.5 partial pressure range using the Brunauer–Emmett– Teller (BET) equation.

## 2.3. Catalytic testing

The catalysts (0.156 g) for catalytic oxidation of HCHO were used in a fixed-bed continuous flow reactor tested at ambient temperature. The Flowing  $\text{N}_2$  through a para-formaldehyde container produced gaseous HCHO. Flowing  $\text{O}_2$  through a water bubbler produced water vapor. At room temperature ( $30^\circ\text{C}$ ), a gas mixture containing 100 sccm pure  $\text{O}_2$ , 90 sccm HCHO/ $\text{N}_2$  (balanced by  $\text{N}_2$ ), and humidified air  $\text{O}_2$  of 50 sccm (this flow rate bubbled through water to maintain relative

humidity of 50%) was provided for the reaction in reactor 0.5 inches diameter and length of 5 inches. Flowing nitrogen through paraformaldehyde in a round-bottomed flask at 40 °C in a water bath produced gaseous HCHO. The feed stream's HCHO content and relative humidity were maintained by adjusting the make-up gas flowrate with GHSV of 35,000 sccm gcat<sup>-1</sup>. In the thoroughgoing procedure, the initial HCHO concentration of 20 ppm is maintained. The formaldehyde elimination efficiency was determined using a Multi-Gas Analyzer (GASERA ONE, Gasear, Finland) using the following formula:

$$C_{\text{HCHO}} = ([\text{HCHO}]_{\text{in}} - [\text{HCHO}]_{\text{out}}) / [\text{HCHO}]_{\text{in}} * 100\%$$

where  $C_{\text{HCHO}}$  represent removal efficiency,  $[\text{HCHO}]_{\text{in}}$  formaldehyde initial concentration, and  $[\text{HCHO}]_{\text{out}}$  represent final concentration the formaldehyde.

The CO<sub>2</sub> yield was defined as follows:

$$\text{CO}_2 \text{ Yield (\%)} = [\text{CO}_2]_{\text{out}} / [\text{HCHO}]_{\text{in}} * 100\%$$

where  $[\text{HCHO}]_{\text{in}}$  denotes the HCHO concentrations in the inlet, and  $[\text{CO}_2]$  denotes the CO<sub>2</sub> concentration at the output.

### 3. Results and discussion

#### 3.1. Calcination temperature Effect

The thermal stability of the MnO<sub>x</sub> catalyst precursor (MnCO<sub>3</sub>) was investigated using thermogravimetry/DSC (TG/DSC) curves, as illustrated in Fig. 01. TGA was performed in the temperature range of ambient temperature to 900 °C in argon environment to investigate thermal stability and the presence of water in co-precipitation routed MnCO<sub>3</sub>. Weight loss may be classified into three types. Also, the purpose of the thermal gravimetric investigation was to examine how Ag nanoparticles doped on MnO<sub>x</sub> varied in thermal behavior from undoped MnO<sub>x</sub>. Weight loss below 300 °C is caused by the removal of physically adsorbed water and the desorption of chemically bonded water. Notice that the weight loss in MnCO<sub>3</sub> below 350°C is 7%. In the temperature range of 300 to 480 °C, a rapid reduction in weight loss of about 30% is seen, which may be attributed to the conversion of metal carbonate to metal oxides and the evolution of CO<sub>2</sub> gas. The growth of lattice oxygen and the phase change from MnCO<sub>3</sub> to MnO<sub>2</sub>

to  $\text{Mn}_2\text{O}_3$  to  $\text{Mn}_3\text{O}_4$  when the temperature rises to  $480^\circ\text{C}$ . Notice that the maximum weight loss is shown below  $500^\circ\text{C}$ . There is no weight loss after that until the temperature reaches  $900^\circ\text{C}$ .

When calcined at elevated temperatures,  $\text{MnO}_x$  tended to lose carbon dioxide and oxygen ( $\text{MnCO}_3 \rightarrow \text{MnO}_2 \rightarrow \text{Mn}_2\text{O}_3 \rightarrow \text{Mn}_3\text{O}_4$ ), according to the TG/DSC findings. Similarly, the curve of  $\text{Ag/MnO}_x$  is also shown and clearly indicating that  $\text{MnO}_x$  less weight loss is decreased after the doping the Ag. The TGA indicates a progressive degradation phase with an initiation temperature of  $50^\circ\text{C}$  when the same conditions are applied to the research of an  $\text{Ag/MnO}_x$  catalyst, which is attributed to volatile impurities and moisture breakdown. Until the catalyst reaches a temperature of  $370^\circ\text{C}$ , it does not lose weight. There is rapid weight loss in the temperature range of  $380\text{--}480^\circ\text{C}$ . There was a 28% loss in this region. As a result, the catalyst may be assumed to be thermally stable up to  $400^\circ\text{C}$ , with a significant loss in thermal stability as the temperature rises. The  $\text{Ag/MnO}_x$  is more thermally stable as shown.

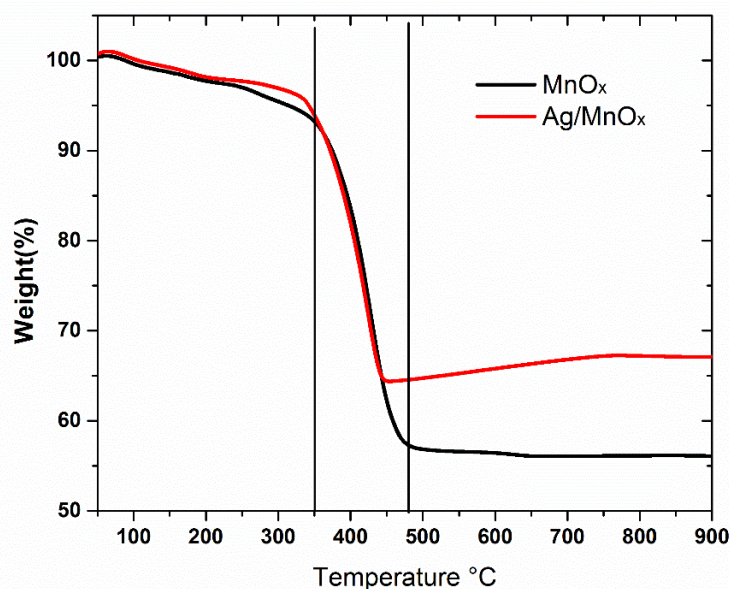


Fig. 01: TGA analysis

### 3.2. Structural analysis

XRD was used to identify the crystalline phase of as-prepared samples (Fig. 02). Both the catalyst shows the peak  $18.2(101)$ ,  $29.2(112)$ ,  $31.1(200)$ ,  $32.6(103)$ ,  $36.6(202)$ ,  $38.3(009)$ ,  $44.6$ ,  $51.3$ ,  $58.7(321)$ ,  $60.1(224)$ ,  $64.9(400)$  show the differential peaks of tetragonal Hausmanite  $\text{Mn}_3\text{O}_4$  (JCPDS 008-0017). In the diffraction peaks some of peaks  $27.4(111)$ ,  $46.4(210)$ ,  $56.1(211)$ ,  $68.5(211)$ ,  $69.8(102)$  are the differential peaks of  $\text{MnO}_2$  (JCPDS 024—0735). It is pyrolusite in nature There



are no Ag crystalline phases for the catalysts, indicating that Ag is evenly distributed in the MnOx support. All the peak intensity of Ag/MnO<sub>2</sub> gets high intensity when Ag is added. Their small peak widths and strong intensities indicate great crystallinity of Ag/MnOx. There are also some peaks shifts in Xrd after adding Ag which is indicated that the dopant was successfully incorporated.

### 3.3. BET Analysis

The surface area of the as-synthesized catalysts was examined using BET surface area analysis to measure the surface area and evaluate the relationship between surface area and catalytic activity for the oxidation of HCHO. N<sub>2</sub> adsorption-desorption experiments showed the pore size, surface area and total porosity (total surface pore volume) of both synthesized nanostructures as shown in Table. 01. The surface area of the un-doped catalyst MnOx was around 22.431 m<sup>2</sup> g<sup>-1</sup> and exhibited 88% HCHO conversion, but after doping Ag nanoparticles, i.e., Ag/MnOx, the surface area has been significantly increased to 30.481 m<sup>2</sup> g<sup>-1</sup> and the HCHO conversion has been significantly increased to 94 %.

The presence of Ag NPs on the surface of MnOx is responsible for the significant increase in surface areas. The surface area is increased from 26.731 m<sup>2</sup> g<sup>-1</sup> to 32.481 m<sup>2</sup> g<sup>-2</sup>. The BJH formula from the N<sub>2</sub> adsorption isotherms desorption branch was used to calculate the average pore size. Both the catalyst shows the average pore diameter of 10.18 nm and 10.18 nm which indicated that the difference in the catalyst efficacy is due to different surface area.

Table 01: BET analysis of Samples

| Sample (nm) | Surface area(m <sup>2</sup> /g) | Pore volume (cm <sup>3</sup> /g) | Average pore diameter |
|-------------|---------------------------------|----------------------------------|-----------------------|
| MnOx        | 22.731                          | 0.1319                           | 10.18                 |
| Ag/MnOx     | 30.481                          | 0.1704                           | 10.18                 |

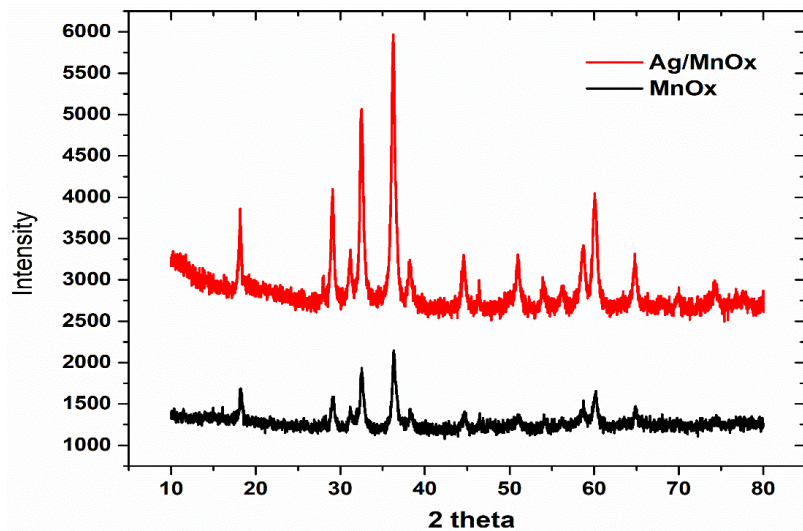


Fig. 02: XRD patterns

### 3.4. Catalytic oxidation of HCHO

The as-obtained MnO<sub>2</sub> and Ag/MnO<sub>2</sub> was used for the catalytic oxidation of formaldehyde at room temperature (30 °C), and the results are shown in Fig. 03. Both catalysts exhibited superior activity for formaldehyde removal with efficiencies more than 70% at the initial stage (first 20 min). As the time passes, Ag/MnO<sub>x</sub> maintained a high catalytic activity of ca. 91% while MnO<sub>2</sub> started to decline the removal efficiency after 40min. The maximum removal efficiency of MnO<sub>2</sub> 88% after 40 minutes. After that MnO<sub>x</sub> catalyst start to deactivation. The main reason of deactivation is the adsorption of intermediate and H<sub>2</sub>O. Notice that CO<sub>2</sub> production begins to decline sharply at 60 minutes and then begins to rise again up to 100 minutes. HCHO conversions on Ag/MnO<sub>x</sub> are diminishing, which might be related to the buildup of intermediate species or changes in active species on the catalyst surface. The major intermediates in HCHO oxidation are dioxymethylene (DOM) and HCOO species, which are mostly adsorbed on the MnO<sub>x</sub> surface. It is demonstrated that the composition and reactivity of active species have a significant impact on the production and transformation of intermediate species. As a result, activity variations and the emergence of an inflection point on Ag/MnO<sub>x</sub> catalysts should be due to changes in active species [20], [23], [26], [40]. The maximum removal efficiency of 94%. The removal efficiency is shown in Fig. 04. After 100 minutes Ag/MnO<sub>2</sub> also start deactivation have same reason of deactivation of MnO<sub>2</sub>. The CO<sub>2</sub> produced by formaldehyde oxidation across various MnO<sub>x</sub> and Ag/MnO<sub>x</sub> catalysts throughout the reaction is shown in fig. In the beginning, the produced CO<sub>2</sub> over MnO<sub>x</sub> and Ag/MnO<sub>2x</sub> was around 15.02 ppm and 14.369 ppm, respectively, and then

progressively decreased to 3.1 ppm and 3.5 ppm as the reaction progressed for 250 minutes. The result indicates that Ag/MnOx is more favorable for the catalytic oxidation of HCHO as it is more thermally stable, high crystallinity and high surface area. It is proposed that Ag nanostructure improve the removal efficiency.

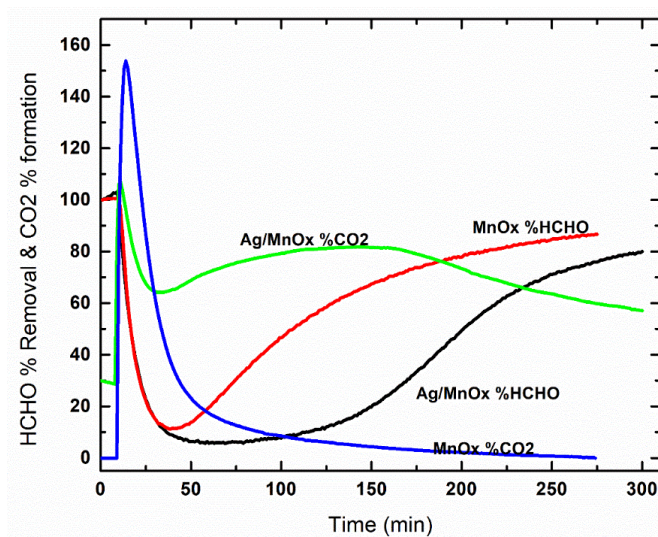


Fig. 03: HCHO removal efficiency as a function of time over MnOx and Ag/MnOx

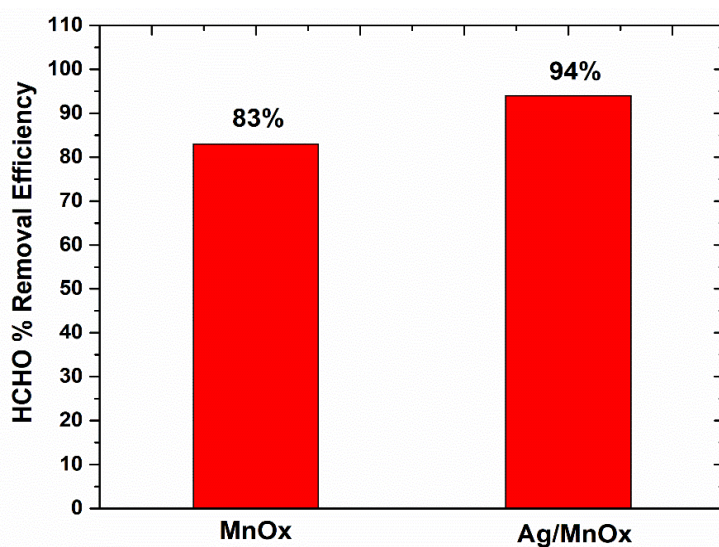


Fig. 04: HCHO % Removal Efficiency

#### 4. Conclusions

In conclusion, we described a technique for preparing MnOx and Ag/MnOx by adding Ag to a co-precipitation process. An Ag/MnOx is favorable for the removal of HCHO due its high crystallinity, high thermally stability. At ambient temperature, this kind of Ag/MnOx was very

effective for HCHO oxidation, converting 20 ppm HCHO at 30 °C under a WHSV of 35000 scm gcal<sup>-1</sup>. The inclusion of Ag nanostructure in MnOx was essential for generating high surface area and surface-active sites, which allowed HCHO to be converted to intermediates effectively. This research presents a co-precipitation method for synthesizing crystallized Ag/MnOx for effective HCHO oxidation, as well as identifying active sites for the transformation of the reactant and intermediates, allowing for the rational design of MnOx for HCHO oxidation with long-term activity and high stability.

## References

1. Bai, B. and *et al.*. Progress in research on catalysts for catalytic oxidation of formaldehyde. *Cuihua Xuebao/Chinese J. Catal.*, 2016. 37(1): P. 102–122.
2. Zhu, S. and *et al.*. Progress of Catalytic Oxidation of Formaldehyde over Manganese Oxides. *ChemistrySelect.*, 2019. 4(41): P. 12085–12098.
3. Ye, J. and *et al.*. Room-temperature formaldehyde catalytic decomposition. *Environ. Sci. Nano*, 2020 7(12): P. 3655–3709
4. Nie, L. and *et al.*. Room-temperature catalytic oxidation of formaldehyde on catalysts. *Catal. Sci. Technol.*, 2016. 6(11): P. 3649–3669
5. Vellingiri, K. and *et al.*. Advances in thermocatalytic and photocatalytic techniques for the room/low temperature oxidative removal of formaldehyde in air. *Chem. Eng. J.*, 2020. 399: P. 125759.
6. Shao, Y. and *et al.*, Biotechnology progress for removal of indoor gaseous formaldehyde. *Appl. Microbiol. Biotechnol.*, 2020. 104(9): P. 3715–3727.
7. Guo, Y. and *et al.*. Recent advances in VOC elimination by catalytic oxidation technology onto various nanoparticles catalysts: a critical review. *Appl. Catal. B Environ.*, 2021. 281: P. 119447.
8. Peng, C. and *et al.*. Recent advances in the preparation and catalytic performance of Mn-based oxide catalysts with special morphologies for the removal of air pollutants. *J. Mater. Chem. A*. 2021. 9(22): P. 12947–12980.
9. Yusuf, A. and *et al.*. Advances on transition metal oxides catalysts for formaldehyde oxidation: A review. *Catal. Rev. Sci. Eng.*, 2017. 59(3): P. 189–233.
10. Zhou, J. and *et al.*. Oriented growth of layered-MnO<sub>2</sub> nanosheets over A-MnO<sub>2</sub> nanotubes for enhanced room-temperature HCHO oxidation, 2017. 207.

11. Guan, S. and *et al.*. A review of the preparation and applications of MnO<sub>2</sub> composites in formaldehyde oxidation. *The Korean Society of Industrial and Engineering Chemistry*, 2018.
12. Guo, J. and *et al.*. Review on noble metal-based catalysts for formaldehyde oxidation at room temperature. *Appl. Surf. Sci.*, 2018. 475: P. 237–255.
13. Bai, B. and *et al.*. Positive effects of K<sup>+</sup> ions on three-dimensional mesoporous Ag/Co<sub>3</sub>O<sub>4</sub> catalyst for HCHO oxidation. *ACS Catal.*, 2014. 4(8): P. 2753–2762.
14. Qu, Z. and *et al.*. Highly active Ag/SBA-15 catalyst using post-grafting method for formaldehyde oxidation. *J. Mol. Catal. A Chem.*, 2012. 356: P. 171–177.  
Zhang, L. and *et al.*. Mn-promoted Ag supported on pure siliceous Beta zeolite (Ag/Beta-Si) for catalytic combustion of formaldehyde, *Appl. Catal. B Environ.*, 2020. 268: P. 118461.
15. Huang *et al.*, Catalytically Active Single-Atom Sites Fabricated from Silver Particles. *Angew. Chemie Int. Ed.*, 2012. 51(17): P. 4198–4203
16. Yu, L. and *et al.*. Ag supported on CeO<sub>2</sub> with different morphologies for the catalytic oxidation of HCHO. *Chem. Eng. J.*, 2018. 334: P. 2480–2487.
17. Tang, X. and *et al.*. Complete oxidation of formaldehyde over Ag/MnO<sub>x</sub>-CeO<sub>2</sub> catalysts,” *Chem. Eng. J.*, 2006. 118(1–2): P. 119–125.
18. Tang, X. and *et al.*. Pt/MnO<sub>x</sub>-CeO<sub>2</sub> catalysts for the complete oxidation of formaldehyde at ambient temperature. *Appl. Catal. B Environ.*, 2008. 81(1–2): P. 115–121.
19. An, N. and *et al.*. Complete oxidation of formaldehyde at ambient temperature over supported Pt/Fe<sub>2</sub>O<sub>3</sub> catalysts prepared by colloid-deposition method. *J. Hazard. Mater.*, 2011. 186(2–3): P. 1392–1397.
20. An, N. and *et al.*, Catalytic oxidation of formaldehyde over different silica supported platinum catalysts. *Chem. Eng. J.*, 2013. 215–216: P. 1–6.
21. V. A. De La Peña O’Shea, M. C. Álvarez-Galván, J. L. G. Fierro, and P. L. Arias, Influence of feed composition on the activity of Mn and PdMn/Al<sub>2</sub>O<sub>3</sub> catalysts for combustion of formaldehyde/methanol. *Appl. Catal. B Environ.*, 2005. 57(3): P. 191–199.
22. L. Zhang *et al.*, Complete oxidation of formaldehyde at room temperature over an Al-rich Beta zeolite supported platinum catalyst. *Appl. Catal. B Environ.*, 2017. 219: P. 200–208.
23. Park, S. J. Oxidation of formaldehyde over Pd/Beta catalyst. *Chem. Eng. J.*, 2012. 195–196: P. 392–402.
24. Li, C. and *et al.*. Catalytic combustion of formaldehyde on gold/iron-oxide catalysts. *Catal.*

- Commun.*, 2008. 9(3): P. 355–361.
25. Zhang, Y. and *et al.*, Gold catalysts supported on the mesoporous nanoparticles composed of zirconia and silicate for oxidation of formaldehyde. *J. Mol. Catal. A Chem.*, 2009. 316(1–2): P. 100–105.
  26. B. Liu *et al.*, Investigation of catalytic mechanism of formaldehyde oxidation over three-dimensionally ordered macroporous Au/CeO<sub>2</sub> catalyst. *Appl. Catal. B Environ.*, 2012. 111–112: P. 467–475.
  27. Ma, C. and *et al.*. Investigation of formaldehyde oxidation over Co<sub>3</sub>O<sub>4</sub>-CeO<sub>2</sub> and Au/Co<sub>3</sub>O<sub>4</sub>-CeO<sub>2</sub> catalysts at room temperature: Effective removal and determination of reaction mechanism *Environ. Sci. Technol.*, 2011. 45(8): P. 3628–3634.
  28. Wen, Y. and *et al.*. Impact of synthesis method on catalytic performance of MnO<sub>x</sub>-SnO<sub>2</sub> for controlling formaldehyde emission. *Catal. Commun.*, 2009. 10(8): P. 1157–1160.
  29. Wang, Y. and *et al.*. Three-dimensional ordered mesoporous Co-Mn oxide: A highly active catalyst for ‘storage-oxidation’ cycling for the removal of formaldehyde. *Catal. Commun.*, 2013. 36: P. 52–57.
  30. Chen, H. and *et al.*. Self-assembly of novel mesoporous manganese oxide nanostructures and their application in oxidative decomposition of formaldehyde. *J. Phys. Chem. C*, 2007. 111(49): P. 18033–18038.
  31. LIU, X. and *et al.*. A comparative study of formaldehyde and carbon monoxide complete oxidation on MnO<sub>x</sub>-CeO<sub>2</sub> catalysts. *J. Rare Earths*, 2009. 27(3): P. 418–424.
  32. Sekine, Y. Oxidative decomposition of formaldehyde by metal oxides at room temperature. *Atmos. Environ.*, 2002. 36(35): P. 5543–5547.
  33. Chen, T. and *et al.*. Tunnel structure effect of manganese oxides in complete oxidation of formaldehyde. *Microporous Mesoporous Mater.*, 2009. 122(1–3): P. 270–274.
  34. Miao, L. and *et al.*. Review on manganese dioxide for catalytic oxidation of airborne formaldehyde. *Appl. Surf. Sci.*, 2018. 466: P. 441–453.
  35. Li, X. and *et al.*. High-efficient degradation of benzene over Pt/TiO<sub>2</sub> by adding a small amount of H<sub>2</sub> under a mild condition. *Catal. Commun.*, 2011. 12(7): P. 621–624.
  36. Eguizábal, A. and *et al.*. Pt based catalytic coatings on poly(benzimidazole) micromonoliths for indoor quality control. *Catal. Today*, 2015. 241: P. 114–124.
  37. He, D. and *et al.*. Catalytic combustion of volatile organic compounds over CuO-CeO<sub>2</sub>

- supported on SiO<sub>2</sub>-Al<sub>2</sub>O<sub>3</sub> modified glass-fiber honeycomb. *Ranliao Huaxue Xuebao/Journal Fuel Chem. Technol.*, 2017. 45(3): P. 354–361.
38. Facile Controlled Synthesis of Pt/MnO<sub>2</sub> Nanostructured Catalysts and Their Catalytic Performance for Oxidative Decomposition of Formaldehyde.
  39. Li, H. F.N. and *et al.*. High surface area Au/CeO<sub>2</sub> catalysts for low temperature formaldehyde oxidation. *Appl. Catal. B Environ.*, 2011. 110: P. 279–285.
  40. Hu, P. and *et al.*. Surface-confined atomic silver centers catalyzing formaldehyde oxidation. *Environ. Sci. Technol.*, 2015. 49(4): P. 2384–2390.
  41. Qu, Z. and *et al.*. High catalytic activity for formaldehyde oxidation of AgCo/APTES@MCM-41 prepared by two steps method. *Appl. Catal. A Gen.*, 2014. 487: P. 100–109.
  42. Zhang J. and *et al.*. Effect of Support on the Activity of Ag-based Catalysts for Formaldehyde Oxidation. *Sci. Rep.*, 2015. 5: P. 1–10.
  43. Kumar, A. and *et al.*. In situ conversion of manganese carbonate to manganese oxide/hydroxide and its supercapacitive analysis in aqueous KOH solution. *Ionics (Kiel)*, 2017. 23.(12): P. 3409–3418.
  44. Li, X. and *et al.*. Facile synthesis of Ag-modified manganese oxide for effective catalytic ozone decomposition. *J. Environ. Sci. (China)*, 2019. 80: P. 159–168.
  45. Adil, S. F. and *et al.*. Nano silver-doped manganese oxide as catalyst for oxidation of benzyl alcohol and its derivatives: Synthesis, characterisation, thermal study and evaluation of catalytic properties. *Oxid. Commun.*, 2013. 36(3): P. 778–791.
  46. Assal M. E. and *et al.*. Silver-doped manganese based nanocomposites for aerial oxidation of alcohols. *Mater. Express*, 2018. 8(1): P. 35–54.
  47. Catalytic oxidation of formaldehyde over manganese oxides with different crystal structures.”
  48. Zhang, J. and *et al.*. Catalytic oxidation of formaldehyde over manganese oxides with different crystal structures. *Catal. Sci. Technol.*, 2015. 5(4): P. 2305–2313.